Anharmonicity-assisted multiphonon transitions between distant levels in semiconductor quantum dots

I. A. Dmitriev[1,2,3,4] and R. A. Suris[4]

[1]*Max Planck Institute for Solid State Research, 70569 Stuttgart, Germany*

[2]*Institut für Theorie der kondensierten Materie, Karlsruhe Institute of Technology, 76128 Karlsruhe, Germany*

[3]*Institut für Nanotechnologie, Karlsruhe Institute of Technology, 76021 Karlsruhe, Germany*

[4]*A. F. Ioffe Physical-Technical Institute, 194021 St. Petersburg, Russia*

(Received 13 January 2014; revised manuscript received 30 August 2014; published 17 October 2014)

We calculate the multiphonon transition rate from the excited state of a single-occupied two-level quantum dot. The electron interacts with certain optical phonon modes which in turn transfer the transition energy to the bath of other phonon modes decoupled from the electron states. Our theory covers the previously unexplored range of transition energies several times larger than the optical phonon energy and systematically studies the role of quantum interference of the processes involving different virtual polaron states.

DOI: 10.1103/PhysRevB.90.155431 PACS number(s): 73.63.Kv, 71.38.−k, 72.10.Di

I. INTRODUCTION

Recent proposals for optoelectronic implementations of quantum dots (QDs), in particular, for quantum cascade lasers (QCLs), rely on the possibility to efficiently control the nonradiative decay in QDs which is absent in conventional planar heterostructures [1–6]. The optical gain of conventional QCLs in quantum well heterostructures [7,8] is limited by inevitably fast electron transitions due to emission of longitudinal optical (LO) phonons [9,10]. Indeed, in quantum wells single-phonon transitions are inherently fast due to the continuous energy spectrum of the carrier in-plane motion. By contrast, in QDs with a discrete electronic spectrum such single-phonon transitions would require a perfect match between the level separation and the energy of nearly dispersionless LO phonons [11,12]. In fact, even in the resonant conditions single-phonon transitions are not possible due to avoided crossing of mixed states involving the electron states and LO phonons [13–18]. Over the last decade it was established both theoretically and experimentally that the energy relaxation in QDs is rather due to multiphonon processes which require the anharmonic decay of involved LO phonons [19–27]. It was also demonstrated that quantum confinement of carriers in quantum well QCLs by application of a strong perpendicular magnetic field indeed improves the laser characteristics; in particular, it enables a higher operation temperature [28].

More specifically, in self-assembled QDs which are typically about 10 nm in size and have quantization energies comparable to the Debye energy, there are severe phase-space restrictions on the wave vectors q of phonons interacting with electrons in QDs,

$$q \lesssim \pi/a_{\mathrm{QD}} \ll \pi/a_0, \tag{1.1}$$

where $a_{\mathrm{QD}} \sim 10$ nm is the characteristic scale of the electron wave function and $a_0 \sim 0.5$ nm the lattice constant. The condition (1.1) is particularly strong in QDs where, unlike quantum wires or quantum wells, all three components of q should be small [11]. As a result, (i) single-phonon transitions involving acoustic phonons are only possible for transition energies not exceeding a few meV; (ii) dispersion of relevant optical phonon modes can be safely neglected; (iii) higher-order processes involving direct electron-phonon couplings are also suppressed due to the phase-space limitation (1.1). By contrast, anharmonic phonon-phonon interaction is not restricted by Eq. (1.1). It involves all phonon modes and remains strong [23] [for instance, in GaAs the lifetime $w(1)$ of the Γ-point LO phonon is 7 ps at 77 K and 3.5 ps at 300 K]. This makes the anharmonicity-assisted multiphonon transitions the dominant channel of relaxation in QDs with level spacing exceeding several meV.

So far, both experimental and theoretical studies of the anharmonicity-assisted transitions in QDs have been concentrated on the region of transition energies close to the resonance with the optical phonon energy. It was established [25–27] that the transition probability factorizes in two parts, one describing the anharmonic interaction of a Γ-point LO phonon with the bath of other phonons, and the other the resonant interaction of electronic states with certain LO modes either single-occupied or not occupied by phonon. The electronic part can be calculated, e.g., with the help of the Davydov transformation method [26], while the anharmonicity factor can be calculated numerically using the methods developed for bulk semiconductors [29,30]. Existing theory reasonably well reproduces experimental results for the region of transition energies not far from the optical phonon energy [19–22]. In this range, the energy relaxation rate is of the order of the LO phonon lifetime $w(1)$.

The main purpose of present work is to develop a microscopic theory of electronic relaxation for a broader range of transition energies (including the level separation of several LO phonon energies) where in particular the Davydov transformation method [26] is no longer applicable. In this range of transition energies, powerful approaches developed earlier for the description of multiphonon processes in impurity centers in semiconductors [31–33] also do not provide reliable results since the characteristic frequencies of the lattice and electronic excitations are of the same order of magnitude. Based on the adiabatic approximation, these methods are more suitable for interband processes, for instance, for study of the exciton dephasing and relaxation [34,35].

The paper is organized as follows. In Sec. II we introduce the spectrum and wave functions of a 2-level QD coupled to LO phonons. Section III introduces the anharmonicity which

provides a coupling of the involved LO phonon modes to the bath of lattice vibrations thus making the energy relaxation possible. Our central results are obtained in Sec. IV where the energy relaxation rates are calculated for transition energies not too close to a multiple of the LO phonon energy (the off-resonant relaxation). Here we systematically study the role of quantum interference of the processes involving different virtual polaron states. The energy relaxation in the vicinity of resonances is addressed in Sec. V. In Sec. VI we discuss the main results and illustrate them for a particular model of anharmonic decay. A short summary is given in Sec. VII.

II. POLARON STATES IN A TWO-LEVEL SYSTEM

A. Electron-phonon interaction

We consider an electron in a two-level system (2LS) represented by two orthogonal electron states $|k\rangle = |1\rangle, |2\rangle$ with energies $\varepsilon_k^{(0)}$ (we assume $\varepsilon_2^{(0)} > \varepsilon_1^{(0)}$). The states are coupled to dispersionless LO phonons of frequency Ω. In this section we present the spectrum and wave functions of polaron states in such a system in the absence of lattice anharmonicity. The anharmonicity, which makes real transitions between the polaron states possible, is introduced in Sec. III.

The Hamiltonian of the system H reads

$$H = H_e + \frac{\hbar\Omega}{2}\sum_q [(x_q^\dagger x_q + \partial_q^\dagger \partial_q) I + 2U(q) x_q], \tag{2.1}$$

$$H_e = \begin{pmatrix} \varepsilon_1^{(0)} & 0 \\ 0 & \varepsilon_2^{(0)} \end{pmatrix}, \quad U(q) = \begin{pmatrix} u_{11}^*(q) & u_{12}^*(q) \\ u_{21}^*(q) & u_{22}^*(q) \end{pmatrix}. \tag{2.2}$$

Here I is the identity matrix; the dimensionless operators x_q and ∂_q are expressed in terms of the phonon creation and annihilation operators $b_q^\dagger$ and b_q as $x_q = (b_q + b_{-q}^\dagger)/\sqrt{2}$ and $\partial_q = (b_{-q} - b_q^\dagger)/\sqrt{2}$. It follows that $x_q = x_{-q}^\dagger$, $\partial_q = -\partial_{-q}^\dagger$, and $\partial_q x_p - x_q \partial_p = \delta_{q,p}$. The Fröhlich coupling coefficients $u_{kl}(q) = u_{lk}(q) = u_{kl}^*(-q)$ are given by

$$u_{kl}(q) = \frac{e}{q}\sqrt{\frac{4\pi}{V\epsilon\hbar\Omega}} \int d^3r\, \Psi_k(\mathbf{r})\, \Psi_l(\mathbf{r})\, e^{-i\mathbf{qr}}, \tag{2.3}$$

where ϵ is the effective permittivity of the media [we choose a gauge where $\Psi_k(r)$ are real]. According to Eq. (2.3), the electron in 2LS interacts with phonon modes with very small wave vectors, see Eq. (1.1), which allows us to neglect the optical phonon dispersion.

In Eq. (2.1), it is convenient to use the vector notation $\mathbf{x} \equiv \{x_q\}$, $\boldsymbol{\nabla} \equiv \{\partial_q\}$, $\mathbf{u}_{kl} \equiv \{u_{kl}(q)\}$, with the scalar product $\mathbf{a}\cdot\mathbf{b} \equiv \sum_q a_q^\dagger b_q$. Denoting $\mathbf{a}^2 \equiv \mathbf{a}\cdot\mathbf{a}$, we obtain the following form of $\tilde{H} \equiv H/\hbar\Omega$:

$$\tilde{H}_{kk} = \varepsilon_k + 1/2[(\mathbf{x} + \mathbf{u}_{kk})^2 + \boldsymbol{\nabla}^2], \tag{2.4}$$

$$\tilde{H}_{12} = \tilde{H}_{21} = \mathbf{u}_{12}\cdot\mathbf{x}, \tag{2.5}$$

where $\mathbf{u}_{ik}\cdot\mathbf{x} = \mathbf{x}\cdot\mathbf{u}_{ik}$, and dimensionless

$$\varepsilon_k = \varepsilon_k^{(0)}/\hbar\Omega - \mathbf{u}_{kk}^2/2. \tag{2.6}$$

We assume the polaron energy shift $\hbar\Omega\,\mathbf{u}_{kk}^2/2 \simeq e^2/\epsilon a_{\mathrm{QD}}$ to be small compared to $\hbar\Omega$.

B. Polaron states in decoupled system

In the absence of coupling between the 2LS states, $\mathbf{u}_{12} = 0$, the Hamiltonian (2.4) in each state $|k\rangle$ yields the eigenstates $|k\rangle|\nu_k\rangle$ of the shifted harmonic oscillator,

$$\tilde{H}_{kk}|\nu_k\rangle = \varepsilon_{k\nu}|\nu_k\rangle, \tag{2.7}$$

$$\varepsilon_{k\nu} = \varepsilon_k + \nu + 1/2, \tag{2.8}$$

$$|\nu_k\rangle = \exp(\mathbf{u}_{\mathbf{kk}}^*\cdot\boldsymbol{\nabla})|\nu\rangle. \tag{2.9}$$

Here $|\nu\rangle$ is an eigenstate of free-phonon Hamiltonian $\tilde{H}_{ph} = (\mathbf{x}^2 + \boldsymbol{\nabla}^2)/2$ with total number of phonons ν. The translation operator $e^{\mathbf{u}^*\cdot\boldsymbol{\nabla}}\mathbf{x} = (\mathbf{x} + \mathbf{u})e^{\mathbf{u}^*\cdot\boldsymbol{\nabla}}$ transforms Eq. (2.4) into $\tilde{H}_{ph}$: $e^{-\mathbf{u}_{\mathbf{kk}}^*\cdot\boldsymbol{\nabla}}\tilde{H}_{kk}e^{\mathbf{u}_{\mathbf{kk}}^*\cdot\boldsymbol{\nabla}} = \varepsilon_k + \tilde{H}_{ph}$.

In each state $|k\rangle$ of the 2LS the electron interacts with a definite single phonon mode. Indeed, in the absence of phonon dispersion one can choose the phonon basis $\{\alpha\}$ such that for all $\alpha \neq k$ the scalar product $\mathbf{x}_\alpha\cdot\mathbf{u}_{kk} = 0$ while $\mathbf{x}_k\cdot\mathbf{u}_{kk} \neq 0$. Explicitly, in the old q basis the displacement operator $\mathbf{x}_k$ is given by $\mathbf{x}_k = \mathbf{u}_{kk}(\mathbf{u}_{kk}\cdot\mathbf{x})/\mathbf{u}_{kk}^2$, and the corresponding $\boldsymbol{\nabla}_k = \mathbf{u}_{kk}(\mathbf{u}_{kk}\cdot\boldsymbol{\nabla})/\mathbf{u}_{kk}^2$. In the α basis, the Hamiltonian naturally divides into two parts, $\tilde{H}_{kk} = \tilde{H}_{kk}^{(k)} + \tilde{H}_{ph}^{(\alpha\neq k)}$, where $\tilde{H}_{ph}^{(\alpha\neq k)}$ is the free-phonon Hamiltonian for all modes excluding $\alpha = k$, and $\tilde{H}_{kk}^{(k)} = \varepsilon_k + (x_k + u_{kk})^2/2 - \partial_k^2/2$ describes interaction of the electron in state k with the "phonon eigenmode" $\alpha = k$. Note that in this natural representation $x_k = x_k^\dagger$, $\partial_k = -\partial_k^\dagger$, and $u_{kk} \equiv \sqrt{\mathbf{u}_{kk}^2}$ is a positive real number.

C. Hybridized polaron states

For $\mathbf{u}_{12} \neq 0$, the nondiagonal part (2.5) of the Hamiltonian leads to hybridization of the polaron states $|1\rangle|\mu_1\rangle$ and $|2\rangle|\nu_2\rangle$. Analogously to the case of two independent electronic levels, one can specify a subspace $\mathcal{X}$ of phonon modes such that only phonons from $\mathcal{X}$ interact with electron in 2LS [16]. In addition to the two modes generated by $\mathbf{u}_{11}$ and $\mathbf{u}_{22}$ (on-site interaction), in the case $\mathbf{u}_{12} \neq 0$ one more mode related to the interlevel coupling appears, with displacement operator $\mathbf{x}_{12} = \mathbf{u}_{12}(\mathbf{u}_{12}\cdot\mathbf{x})/\mathbf{u}_{12}^2$.

In systems with a larger number of involved electronic levels the number of couplings and associated phonon modes increases accordingly; for a detailed discussion see Refs. [16,17]. Concerning the inelastic relaxation process, the minimal 2LS model introduced above enables us to perform explicit analysis of the interference of multiphonon processes involving different virtual states. Despite its fundamental importance, the interference was not properly discussed in this context before [25–27], partially in view of the complexity of more realistic multilevel models of QDs; see discussion in Sec. VI.

In Secs. IV–VI, we use several complementary approximation schemes to calculate the spectrum and wave functions of the hybridized polaron states $|\Psi_{k\nu}\rangle$ which diagonalize the Hamiltonian of the system "electron in 2LS + $\mathcal{X}$ phonons." In particular, when the separation of the electron states in 2LS is not too close to a multiple of $\hbar\Omega$ and $\mathbf{u}_{12}^2 \ll \mathbf{u}_{kk}^2$, one can treat the nondiagonal part (2.5) of the Hamiltonian as a small perturbation. In this case, the spectral corrections are

irrelevant, while the amplitudes are given by

$$|\Psi_{k\nu}\rangle = |k\rangle|\nu_k\rangle + |\underline{k}\rangle \sum_{\mu} |\mu_{\underline{k}}\rangle\, A_{\underline{k}\mu k\nu}, \tag{2.10}$$

$$A_{\underline{k}\mu k\nu} = \frac{\langle \mu_{\underline{k}}|\, \mathbf{u}_{12}\cdot\mathbf{x}\,|\nu_k\rangle}{\varepsilon_{k\nu} - \varepsilon_{\underline{k}\mu}}, \tag{2.11}$$

where $\underline{k} = 1$ (2) for $k = 2$ (1). The matrix elements $A_{\underline{k}\mu k\nu}$ in Eq. (2.11) are in general nonzero for $|\nu - \mu| \neq 1$ due to different lattice distortions $\mathbf{u}_{11}$ and $\mathbf{u}_{22}$ in states $|\nu_1\rangle$ and $|\nu_2\rangle$; see Eq. (2.9). In Eqs. (2.10) and (2.11), the on-site interaction (2.9) is treated exactly (to all orders in $\mathbf{u}_{kk}$), while the nondiagonal part (2.5) is taken into account to first order only. In Sec. IV, the nonresonant coupling of polaronic states will be considered both for $\mathbf{u}_{12}^2 \ll \mathbf{u}_{kk}^2$ and $\mathbf{u}_{12}^2 \sim \mathbf{u}_{11}^2 \sim \mathbf{u}_{22}^2$. Later on, in Sec. V, we address the behavior of the system in the vicinity of resonances $\varepsilon_1 - \varepsilon_2 \simeq N$.

Regardless of the approximation implemented for calculation of $\Psi_{k\nu}$, there exists an orthonormal set of exact hybridized polaron states, the eigenstates of the system "electron in 2LS + $\mathcal{X}$ phonons." Relaxation in such system requires a coupling to the thermal bath $\mathcal{Q}$ which is introduced in next section.

III. ANHARMONIC INTERACTION WITH A PHONON BATH

The anharmonicity of the crystal makes real transitions between the hybridized polaron states possible [23–27]. The $\mathcal{X}$ phonons have a final lifetime due to interaction with a thermal bath of $\mathcal{Q}$ phonons. The latter consists of the LO phonon modes $\{\beta\}$ which do not couple to the electron subsystem, $\mathbf{u}_{ik}\cdot\mathbf{x}_\beta \equiv 0$, and of all optical and acoustic modes belonging to other phonon branches.

The lowest-order anharmonic interaction is given by the product of three displacement operators,

$$H^{(ah)} = \frac{2^{3/2}}{3!} \sum_{1,2,3} V^{(ah)}_{1,2,3} x_1 x_2 x_3, \tag{3.1}$$

where indices $n \equiv \{\eta_n, q_n\}$ denote the phonon branch η_n and wave vector q_n of participating phonons, and operators $x_q = 2^{-1/2}(a_q + a^\dagger_{-q})$ as before. The transition probability between the hybridized polaron states $|i\rangle$ and $|f\rangle$ (with energies ε_i and ε_f) reads

$$W_{i\to f} = \frac{2\pi}{\hbar} \sum_{\beta_i,\,\beta_f} P(\beta_i, T)|\langle f|\langle\beta_f|H^{(ah)}|\beta_i\rangle|i\rangle|^2 \times\delta\big(\varepsilon_i - \varepsilon_f + E_{\beta_i} - E_{\beta_f}\big). \tag{3.2}$$

Here we perform the summation over final states of the phonon bath $\{\beta_f\}$ and thermal average [with the Gibbs weight $P(\beta_i, T)$] over initial states $\{\beta_i\}$. The delta function ensures conservation of total energy in the system "polaron states" + "$\mathcal{Q}$ phonons." The range of validity of the golden-rule approximation (3.2) is discussed in Sec. V.

For any definite choice of the momenta of participating Q phonons, the translational symmetry of $H^{(ah)}$ determines a single term in the sum (3.1) entering the matrix element in Eq. (3.2) such that the total momentum is conserved. In the resulting expression, however, one can neglect the dependence of $|V^{(ah)}|^2$ on the $\mathcal{X}$-phonon momentum $q \sim \pi/a_{\rm QD}$ using that $V^{(ah)}$ changes on a much larger scale $\pi/a_0 \gg \pi/a_{\rm QD}$; see Eq. (1.1). As a result, the probability $W_{i\to f}$ can be represented as

$$W_{i\to f} = 2\langle f|\mathbf{x}|i\rangle^2\, w[(\varepsilon_i - \varepsilon_f)/\hbar\Omega]\,, \tag{3.3}$$

$$w(\Delta) = \sum_{s1,s2=\pm1} \frac{2\pi}{\hbar^2\Omega} \sum_{1,2} \big|V^{(ah)}_{1,2,\mathcal{X}}\big|^2 \times \mathcal{N}_1\mathcal{N}_2\delta[\Delta - (s_1\omega_1 + s_2\omega_2)/\Omega], \tag{3.4}$$

where $s_k = +1$ (-1) corresponds to emission (absorption) of the $\mathcal{Q}$ phonon k of frequency ω_k, and $\mathcal{N}_k = [\exp(\hbar\omega_k/T) - 1]^{-1} + (s_k + 1)/2$ are the occupation factors of $\mathcal{Q}$-phonon modes. The square of the multiphonon transition matrix element $\langle f|\mathbf{x}|i\rangle^2 \equiv \sum_\alpha |\langle f|x_\alpha|i\rangle|^2$ does not depend on the choice of the basis $\{\alpha\}$ in the space of $\mathcal{X}$-phonon modes.

Owing to the smallness of momentum of the $\mathcal{X}$-phonons, the probability (3.3) factorizes into two parts. While $w(\Delta)$ depends on the bath degrees of freedom and on the transition energy Δ, the square of the multiphonon matrix element $\langle f|\mathbf{x}|i\rangle^2$ does not depend on the bath degrees of freedom and carries all relevant information about the polaronic system. The rate of anharmonic decay $w(\Delta)$ describes the process of $\mathcal{X}$-phonon decay with the energy Δ being transferred to the phonon bath. In particular, $w(1)$ is the decay rate of the Γ-point LO phonon in the bulk, which was extensively studied both experimentally and theoretically and is known for the majority of semiconductors (see Refs. [29,30] and references therein). The methods developed for calculations of $w(1)$ can be generalized for evaluation of $w(\Delta)$, which, in general, can have nonzero values in the broad interval $-2 \lesssim \Delta \lesssim 2$. Depending on Δ, different channels of anharmonic interaction can become dominant making the calculation of $w(\Delta)$ a nontrivial task. For GaAs, this problem was recently addressed in several works (see Refs. [21,27]) but comprehensive analysis similar to Refs. [29,30] is still lacking. In certain situations, 4-phonon interaction can become relevant. Evidently, such interaction can be treated on the same footing as the 3-phonon one (3.1). The resulting rate contains the same multiphonon matrix element $\langle f|\mathbf{x}|i\rangle^2$ while the corresponding $w(\Delta)$ is nonzero in a larger interval $|\Delta| \lesssim 3$. In this work, we focus on the calculation of the multiphonon matrix element $\langle f|\mathbf{x}|i\rangle^2$. The results are illustrated in Sec. VI using a phenomenological form of $w(\Delta)$ for a particular LA-LA channel of LO 3-phonon relaxation.

IV. ENERGY RELAXATION AND ELECTRON TRANSFER AWAY FROM RESONANCES

In this section we calculate the multiphonon matrix element $\langle f|\mathbf{x}|i\rangle^2$ in Eq. (3.3), using the perturbative approximation (2.10) for the hybridized polaron states $|i\rangle$ and $|f\rangle$. The results obtained in this way are valid for transition energies Δ not too close to an integer and for small interlevel coupling $\mathbf{u}_{12}^2 \ll \mathbf{u}_{kk}^2$. In next subsection we calculate $\langle f|\mathbf{x}|i\rangle^2$ under the simplifying assumption that all phonon modes in the subspace $\mathcal{X}$ coincide. The general multimode result is obtained in Sec. IV B and implemented for several specific regimes of energy relaxation in Sec. IV C. In Sec. IV D we discuss

modification of results for $\mathbf{u}_{12}^2 \sim \mathbf{u}_{11}^2 \sim \mathbf{u}_{22}^2$. The resonant regimes in the vicinity of integer Δ are considered separately in Sec. V.

A. Single-mode approximation

Using Eq. (2.10) for the hybridized polaron states $|f\rangle = |\Psi_{1\mu}\rangle$ and $|i\rangle = |\Psi_{2\nu}\rangle$, we represent the matrix element $\langle f|\mathbf{x}|i\rangle$ as a sum over intermediate virtual states $|k\rangle|\chi_k\rangle$:

$$\langle\Psi_{1\mu}|\mathbf{x}|\Psi_{2\nu}\rangle = \sum_{\chi} \frac{\langle\mu_1|\mathbf{x}|\chi_1\rangle\langle\chi_1|\mathbf{u}_{12}\cdot\mathbf{x}|\nu_2\rangle}{\Delta_{\chi-\nu}} - \sum_{\chi} \frac{\langle\mu_1|\mathbf{u}_{12}\cdot\mathbf{x}|\chi_2\rangle\langle\chi_2|\mathbf{x}|\nu_2\rangle}{\Delta_{\mu-\chi}}. \quad (4.1)$$

Here we introduced

$$\Delta_{\mu-\nu} = \varepsilon_{2\nu} - \varepsilon_{1\mu} = E - (\mu-\nu), \quad (4.2)$$

where $E = (\varepsilon_2^{(0)} - \varepsilon_1^{(0)})/\hbar\Omega + (u_{22}^2 - u_{11}^2)/2$ is the energy shift between two polaronic ladders in units $\hbar\Omega$.

Now we assume that all three displacement operators $\mathbf{x}_1$, $\mathbf{x}_2$, and $\mathbf{x}_{12}$ of the subspace $\mathcal{X}$ correspond to a single phonon mode. That is, $\mathbf{u}_{ik}\cdot\mathbf{x} \equiv u_{ik}x$, where $x = (b+b^\dagger)/\sqrt{2}$ is the displacement operator of this single mode, and $u_{ik} = \sqrt{\mathbf{u}_{ik}^2}$. Using Eq. (2.9), we have

$$\begin{aligned}\langle\mu_k|x|\nu_k\rangle &= \langle\mu|e^{-u_{kk}\partial}xe^{u_{kk}\partial}|\nu\rangle \\ &= \langle\mu|x-u_{kk}|\nu\rangle \\ &= -u_{kk}\delta_{\mu,\nu} + \sqrt{\frac{\mu}{2}}\delta_{\mu,\nu+1} + \sqrt{\frac{\nu}{2}}\delta_{\nu,\mu+1}, \quad (4.3)\end{aligned}$$

where $\mathbf{u}_{ik}\cdot\boldsymbol{\nabla} \equiv u_{ik}\partial$ and $\partial = (b-b^\dagger)/\sqrt{2}$. Correspondingly, the sum in Eq. (4.1) consists of six terms which we group in pairs with equal energy denominators as illustrated in Figs. 1(a)–1(c),

$$\langle\Psi_{1\mu}|x|\Psi_{2\nu}\rangle = \mathcal{R}_a + \mathcal{R}_b + \mathcal{R}_c. \quad (4.4)$$

For brevity, in Fig. 1 and below we use notation (k,ν) for the states $|k\rangle|\nu_k\rangle$ defined by Eq. (2.10).

The contribution $\mathcal{R}_a$ includes processes involving virtual states $(1,\mu)$ and $(2,\nu)$ [Fig. 1(a)]. The corresponding pair of terms enter Eq. (4.1) with the denominator $\Delta_{\mu-\nu}$ and produce

$$\mathcal{R}_a = \frac{u_{12}u_-}{\Delta_{\mu-\nu}}\langle\mu|\tilde{x}|\nu\rangle. \quad (4.5)$$

Here $u_- \equiv u_{22} - u_{11}$ and

$$\langle\mu|\tilde{x}|\nu\rangle = \langle\mu|e^{-u_{11}\partial}xe^{u_{22}\partial}|\nu\rangle \equiv \langle\mu_1|x|\nu_2\rangle. \quad (4.6)$$

Similarly, both virtual states $(1,\mu-1)$ and $(2,\nu+1)$ enter Eq. (4.1) with the denominator $\Delta_{\mu-\nu-1}$ [Fig. 1(a)] and yield

$$\mathcal{R}_b = \frac{u_{12}/\sqrt{2}}{\Delta_{\mu-\nu-1}}\langle\mu|b^\dagger\tilde{x} - \tilde{x}b^\dagger|\nu\rangle. \quad (4.7)$$

The remaining virtual states $(1,\mu+1)$ and $(2,\nu-1)$ yield

$$\mathcal{R}_c = \frac{u_{12}/\sqrt{2}}{\Delta_{\mu-\nu+1}}\langle\mu|b\tilde{x} - \tilde{x}b|\nu\rangle. \quad (4.8)$$

Using the commutation relations $x\tilde{x} - \tilde{x}x = -u_-\tilde{x}$ and $\partial\tilde{x} - \tilde{x}\partial = \exp(u_-\partial)$ in the sum and difference of the matrix elements entering Eqs. (4.7) and (4.8), we obtain

$$2\Delta_{\mu-\nu-1}\mathcal{R}_b = -u_{12}\langle\mu|u_-\tilde{x} + e^{u_-\partial}|\nu\rangle, \quad (4.9)$$

$$2\Delta_{\mu-\nu+1}\mathcal{R}_c = -u_{12}\langle\mu|u_-\tilde{x} - e^{u_-\partial}|\nu\rangle. \quad (4.10)$$

Equations (4.4), (4.5), (4.9), and (4.10) yield

$$\langle\Psi_{1\mu}|x|\Psi_{2\nu}\rangle = \frac{u_{12}}{\Delta_{\mu-\nu}^2 - 1}\langle\mu|e^{-u_{11}\partial}\left[1 + \frac{u_{11}-u_{22}}{\Delta_{\mu-\nu}}x\right]e^{u_{22}\partial}|\nu\rangle. \quad (4.11)$$

Now we expand exponentials $e^{u_{kk}\partial}$ in powers of $\partial = (b - b^\dagger)/\sqrt{2}$ and obtain, to leading order in $u_{ik} \ll 1$ for each μ and ν,

$$\langle\Psi_{1\mu}|x|\Psi_{2\nu}\rangle = \frac{u_{12}(u_{11}-u_{22})^{|\mu-\nu|}}{\Delta_{\mu-\nu}^2 - 1}\left(1 + \frac{\mu-\nu}{\Delta_{\mu-\nu}}\right)C_{\mu\nu}, \quad (4.12)$$

where the combinatorial coefficient $C_{\mu\nu}$ is expressed in terms of $n \equiv \min\{\mu,\nu\}$ and $N = |\mu-\nu|$ as

$$C_{\mu\nu} = \frac{1}{N!}\sqrt{\frac{(n+N)!}{2^N n!}}. \quad (4.13)$$

Equation (4.12) demonstrates the important role of quantum interference between the pairs of processes (a)–(c) illustrated in Fig. 1: while individual terms entering Eq. (4.1) are of different order in $u_{ik} \ll 1$, the interference leads to cancellation

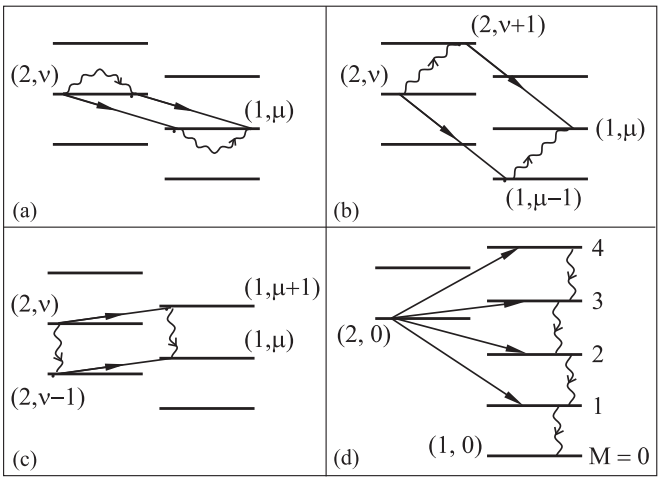

FIG. 1. (a)–(c) Graphical representation of six processes entering the multiphonon matrix element (4.1). Wavy arrows denote the intraladder couplings originating from the anharmonic interaction (3.3), while straight arrows denote the interladder couplings due to the off-diagonal electron-phonon interaction (2.5). Six processes $(2,\nu) \to (1,\mu)$ are grouped into three pairs (a)–(c) each with different energy denominator; see Eqs. (4.5)–(4.8). Due to destructive interference, the contributions (4.5)–(4.8) are of the same order in Fröhlich couplings u_{ik} despite individual terms in Eq. (4.1) being of different order. (d) Illustration of allowed multiphonon transitions entering the sum (4.24) for $E = 2.75$ (straight arrows). In this case, $|\Delta_M| \equiv |E - M| < 2$ for $M = 1,2,3,4$; rare transitions to the intermediate states $(1,M)$ trigger fast intraladder relaxation (4.23) to the ground state (1,0) (wavy arrows). Direct transition to the ground state is impossible since the energy $E = 2.75$ cannot be transferred to the phonon bath in a single 3-phonon collision.

of the leading terms. For instance, from Eq. (4.1) one could naively expect $\langle\Psi_{12}|x|\Psi_{20}\rangle$ to be $O(u_{12})$ since $\langle\mu_k|x|\nu_l\rangle$ are $O(1)$ for $|\mu-\nu|=1$. In fact, the leading contributions cancel, see Eq. (4.7), yielding $\langle\Psi_{12}|x|\Psi_{20}\rangle$ of order $O(u_{12}u_-^2)$ as in Eq. (4.12). As a result of destructive interference, all three pairs (a), (b), and (c) yield contributions of equal order in u_{ik}; see Eq. (4.12).

B. General case

Using the procedure described above for the single-mode case, the vector matrix element (4.1) can be transformed to the following form [compare to Eqs. (4.4)–(4.8)]:

$$\langle\Psi_{1\mu}|\mathbf{x}|\Psi_{2\nu}\rangle=\langle\mu|\frac{\mathbf{u}_-J}{\Delta_{\mu-\nu}}+\frac{\Delta_{\mu-\nu}[\mathbf{x},J]+[\nabla,J]}{\Delta_{\mu-\nu}^2-1}|\nu\rangle, \quad (4.14)$$

where the scalar operator J is given by

$$J=e^{-\mathbf{u}_{11}^*\cdot\nabla}\mathbf{u}_{12}\cdot\mathbf{x}\,e^{\mathbf{u}_{22}^*\cdot\nabla}. \quad (4.15)$$

This operator form of the matrix element is valid for any choice of the basis in the $\mathcal{X}$-phonon subspace.

Generally, vectors $\mathbf{u}_{ik}$ form a linearly independent family, which corresponds to a 3D $\mathcal{X}$-phonon subspace. A convenient $\mathcal{X}$-phonon basis can be constructed using the following orthogonal set of their linear combinations:

$$\mathbf{u}_-=\mathbf{u}_{22}-\mathbf{u}_{11}, \quad (4.16)$$

$$\mathbf{u}_{12,\perp}=\mathbf{u}_{12}-\mathbf{u}_{12,\parallel}, \quad (4.17)$$

$$\mathbf{u}_{\rm out}=\mathbf{u}_+-\mathbf{u}_{+,\parallel}-\mathbf{u}_{+,\perp}. \quad (4.18)$$

Here the subscript $\parallel$ ($\perp$) denotes the component of a given vector which is parallel (perpendicular) to $\mathbf{u}_-$ and lies in the plane formed by vectors $\mathbf{u}_-$ and $\mathbf{u}_{12}$. The vector $\mathbf{u}_{\rm out}$ is formed by the out-of-plane component (4.18) of $\mathbf{u}_+=\mathbf{u}_{22}+\mathbf{u}_{11}$ such that $(\mathbf{u}_{\rm out}\cdot\mathbf{u}_-)=(\mathbf{u}_{\rm out}\cdot\mathbf{u}_{12})=0$. Using the orthonormal set $\{\mathbf{e}_\parallel=\mathbf{u}_-/u_-,\ \mathbf{e}_\perp=\mathbf{u}_{12,\perp}/u_{12,\perp},\ \mathbf{e}_{\rm out}=\mathbf{u}_{\rm out}/u_{\rm out}\}$, we represent the $\mathcal{X}$-phonon operators as $\mathbf{x}=\sum\mathbf{x}_\alpha=\sum\mathbf{e}_\alpha(\mathbf{e}_\alpha\cdot\mathbf{x})$ and $\nabla=\sum\partial_\alpha=\sum\mathbf{e}_\alpha(\mathbf{e}_\alpha\cdot\nabla)$, $\alpha=\{\parallel,\perp,{\rm out}\}$.

The $\mathcal{X}$-phonon basis (4.16)–(4.18) is chosen such that the resulting out-of-plane mode is irrelevant. In fact, it can be neglected by putting $\mathbf{u}_+=0$ from the very beginning. Indeed, physical observables should not change under uniform distortion of the lattice $\mathbf{u}_{kk}\to\mathbf{u}_{kk}+\delta$ as long as the number of electrons in QD is conserved [16]. Therefore, a variation of $\mathbf{u}_+$ should not modify the rate of interlevel transitions in 2LS. In the basis (4.16)–(4.18), the operator (4.15) entering Eqs. (4.14) reads

$$J=e^{u_-\partial_\parallel}(u_{12,\parallel}x_\parallel+u_{12,\perp}x_\perp-\mathbf{u}_{12}\cdot\mathbf{u}_{22}). \quad (4.19)$$

The commutators $[\mathbf{x}_{\rm out},J]=[\partial_{\rm out},J]=0$. Taking into account that $\mathbf{u}_{\rm out}\cdot\mathbf{u}_{12}=0$, one obtains $\langle\Psi_{1\mu}|\mathbf{x}_{\rm out}|\Psi_{2\nu}\rangle=0$. The occupation of the out-of-plane mode does not change also in other components of the multiphonon matrix element. Therefore, the out-of-plane mode can be disregarded as expected.

The initial problem is thus reduced to diagonalization of a 2LS interacting with two harmonic oscillators. Correspondingly, the mixed polaronic states $\Psi_{k\nu}=\Psi_{k\nu_\parallel\nu_\perp}$ are now characterized by the level index k and by two occupation numbers $\{\nu_\parallel,\nu_\perp\}$. As before, $\nu=\nu_\parallel+\nu_\perp$ denotes the sum of occupation numbers of the relevant $\mathcal{X}$-phonon modes.

Using commutation relations $[\nabla,J]=\mathbf{u}_{12}e^{u_-\partial_\parallel}$ and $[\mathbf{x},J]=-\mathbf{u}_-J$, Eq. (4.14) can be rewritten as

$$\langle\Psi_{1\mu}|\mathbf{x}|\Psi_{2\nu}\rangle=\frac{\mathbf{u}_{12}\langle\mu|e^{u_-\partial_\parallel}|\nu\rangle}{\Delta_{\mu-\nu}^2-1}-\frac{\mathbf{u}_-\langle\mu|J|\nu\rangle}{\Delta_{\mu-\nu}\left(\Delta_{\mu-\nu}^2-1\right)}. \quad (4.20)$$

This expression generalizes Eq. (4.11) obtained in the single-mode approximation.

Inspection of Eq. (4.20) gives the following selection rules for the multiphonon transitions:

(1) the change of the occupation number of the first mode $\mu_\parallel-\nu_\parallel$ can be arbitrary;

(2) the occupation number of the second mode may not change or changes by 1, $\mu_\perp-\nu_\perp=0,\pm1$.

Interestingly, since $x_\perp$ enters the last term only in Eq. (4.20), the anharmonic interaction with the second mode does not result in change of its occupation number. This number may change only due to anharmonic interaction with the first mode.

Our goal is to calculate the square of the matrix element $\langle f|\mathbf{x}|i\rangle^2=\sum_\alpha|\langle\Psi_{1\mu}|x_\alpha|\Psi_{2\nu}\rangle|^2$ to the leading order in $\mathbf{u}_{ik}\ll1$. Expanding, as previously, the exponential $e^{u_-\partial_\parallel}$ in powers of $\partial_\parallel$, we obtain for the transitions with $\mu_\perp=\nu_\perp$ (in this case $\mu-\nu=\mu_\parallel-\nu_\parallel$)

$$\langle\Psi_{1\mu_\parallel\nu_\perp}|\mathbf{x}|\Psi_{2\nu_\parallel\nu_\perp}\rangle^2=\frac{u_-^{2N}(n+N)!}{2^Nn!(N!)^2\left(\Delta_{\mu-\nu}^2-1\right)^2}\left[u_{12,\perp}^2+u_{12,\parallel}^2\left(1+\frac{\mu-\nu}{\Delta_{\mu-\nu}}\right)^2\right]. \quad (4.21)$$

In the case $u_{12,\perp}=0$ this expression reduces to Eq. (4.12). For transitions with $\mu_\perp=\nu_\perp\pm1$, the result reads (in this case $\mu-\nu=\mu_\parallel-\nu_\parallel\pm1$)

$$\langle\Psi_{1\mu_\parallel\nu_\perp\pm1}|\mathbf{x}|\Psi_{2\nu_\parallel\nu_\perp}\rangle^2=\max\{\nu_\perp\pm1,\nu_\perp\}\frac{(n+N)!}{2^{N+1}n!(N!)^2}\frac{u_{12,\perp}^2u_-^{2(N+1)}}{\Delta_{\mu-\nu}^2\left(\Delta_{\mu-\nu}^2-1\right)^2}. \quad (4.22)$$

In Eqs. (4.21) and (4.22), $N=|\mu_\parallel-\nu_\parallel|$ and $n\equiv\min\{\mu_\parallel,\nu_\parallel\}$.

C. Energy relaxation

The expression for the transition probability (3.3) together with the matrix elements (4.21) and (4.22) describes the elementary scattering acts between polaron states of *different* ladders, $|\Psi_{1\mu}\rangle\leftrightarrow|\Psi_{2\nu}\rangle$. In addition, it is necessary to consider the anharmonicity-induced *intraladder* transitions. Using Eq. (3.3) and disregarding the interladder interaction (2.5), $|\Psi_{k\nu}\rangle\simeq|k\rangle|\nu_k\rangle$, for the intraladder transitions we have [see Eq. (4.3)]

$$2|\langle\Psi_{k\mu}|x_\alpha|\Psi_{k\nu}\rangle|^2\simeq\sum_\pm\min\{\mu_\alpha,\nu_\alpha\}\delta_{\mu_\alpha,\nu_\alpha\pm1}.$$

This yields the expected result for the transition rate between the neighboring ladder states,

$$W_{(k,\nu_\alpha)\to(k,\nu_\alpha\mp1)}=(\nu_\alpha+1/2\pm1/2)w(\pm1), \quad (4.23)$$

corresponding to creation or annihilation of a phonon in a given $\mathcal{X}$ mode α.

We consider now the energy relaxation of an electron, initially occupying the ground state of the upper polaronic ladder, $|i\rangle = |\Psi_{2,0}\rangle$, to the ground state of the second ladder, $|f\rangle = |\Psi_{1,0}\rangle$. For large energy separation, $E = \varepsilon_2 - \varepsilon_1 > 2$ [see Eq. (4.2)], the relaxation necessarily takes place in several steps: relatively slow interladder transition $|\Psi_{2,0}\rangle \to |\Psi_{1,M}\rangle$ to an intermediate state $|\Psi_{1,M}\rangle$, $M > 0$, triggers fast M-step relaxation $|\Psi_{1,M}\rangle \to |\Psi_{1,0}\rangle$ within the second ladder; see Fig. 1(d). The total energy relaxation rate $\Gamma_0 = W_{(2,0)\to(1,0)}$ is controlled by the slowest transitions and is given by the sum of probabilities of all possible *interladder* processes $|\Psi_{2,0}\rangle \to |\Psi_{1,M}\rangle$.

Using Eqs. (3.3), (4.21), and (4.22), we obtain

$$\begin{aligned}\Gamma_0 &= \sum_M \Gamma_0^{(M)} \\ &= \sum_M 2w(\Delta_M)[\langle\Psi_{1,M,0}|\mathbf{x}|\Psi_{2,0,0}\rangle^2 \\ &\quad + \langle\Psi_{1,M-1,1}|\mathbf{x}|\Psi_{2,0,0}\rangle^2] \\ &= \sum_M \frac{w(\Delta_M)u_-^{2M}}{2^{M-1}M!\left(\Delta_M^2-1\right)^2} \\ &\quad \times\left[u_{12,\perp}^2\left(1+\frac{M}{\Delta_M^2}\right)+u_{12,\parallel}^2\left(1+\frac{M}{\Delta_M}\right)^2\right], \end{aligned} \tag{4.24}$$

where the transition energies $\Delta_M = E - M$, see Eq. (4.2), and the sum is over M in the stripe $|\Delta_M| < 2$ where $w(\Delta_M) \neq 0$. The interladder processes entering Eq. (4.24) are illustrated in Fig. 1(d) for $E = 2.75$. In this case, direct transition $|\Psi_{2,0}\rangle \to |\Psi_{1,0}\rangle$ to the ground state is impossible.

Despite four terms corresponding to different M in Eq. (4.24) being of different order in small parameter u_-, any of these terms can be important since the anharmonic decay rate $w(\Delta_M)$ for different M may differ significantly. In particular, assuming $1 < E < 2$, the $M = 1$ term is important for specific ranges of E where $w(E) \lesssim w(E-1)u_-^2$. Despite $u_-^2 \ll 1$ being small, for such ranges accounting for the leading $M = 0$ term only [25–27] is insufficient even in the range $0 < E < 2$ and small temperature $T \ll \hbar\Omega$, where the direct $M = 0$ transition $|\Psi_{2,0}\rangle \to |\Psi_{1,0}\rangle$ to the ground state of the second ladder generally prevails.

Equation (4.24) correctly describes the energy relaxation at temperatures $T \ll \hbar\Omega$. At such low T, two terms corresponding to $\Delta_M < 0$ can be safely neglected as in this case the anharmonic decay requires the absorption of bath phonons and, therefore, is exponentially suppressed; see Eq. (3.3). At higher temperature, apart from importance of the $\Delta_M < 0$ terms, the intraladder transitions lead to fast thermalization within the states of the upper ladder before the transition to the lower ladder takes place (unless strong hybridization of states of different ladders occurs in the vicinity of resonances; see Sec. V). Accordingly, the expression (4.24) should be modified to include nonzero thermal occupation of excited states $|\Psi_{2,n}\rangle$, which yields

$$\begin{aligned}\Gamma_T &= \sum_{n=0}^{\infty} \frac{\exp(-n\hbar\Omega/T)}{1-\exp(-\hbar\Omega/T)}\Gamma_n, \\ \Gamma_n &= \sum_M \Gamma_n^{(M)} \\ &= \sum_M 2w(\Delta_M)\sum_{k=0}^{n}\sum_{l=0,\pm1} \\ &\quad \times \langle\Psi_{1,M+n-k-l,k+l}|\mathbf{x}|\Psi_{2,n-k,k}\rangle^2, \end{aligned} \tag{4.25}$$

where the matrix elements are given by Eqs. (4.21) and (4.22).

The above results generalize the theory developed previously for the same mechanism of relaxation. In Refs. [13,16,23–27] only the case of relatively small energy separation $E < 2$ was considered and only processes, corresponding to $M = 0$ in Eq. (4.24), were discussed. The leading term of Eq. (4.24),

$$\Gamma_0^{(0)} = \frac{2w(E)u_{12}^2}{(E^2-1)^2}, \tag{4.26}$$

provides the 2LS version of the results of these works away from the resonance $E = 1$. Here the only relevant phonon mode is that generated by $\mathbf{u}_{12}$; thus, only the combination $u_{12,\perp}^2 + u_{12,\parallel}^2 = u_{12}^2$ enters the result. Accordingly, the lowest-order contribution (4.26) reproduces Eq. (4.12) obtained within the single-mode approximation. Modifications of Eq. (4.26) in the resonant case, which was the main emphasis of Refs. [13,16,23–27], are considered in Sec. V.

Next-order terms in electron-phonon interaction become important when $w(E) \lesssim w(E-1)u_-^2$. For $M = 1$, Eq. (4.24) yields a correction to Eq. (4.26) of fourth order in u_{kl} which is relevant for energy separation in the interval $E \equiv \Delta_1 + 1 < 3$:

$$\Gamma_0^{(1)} = \frac{w(\Delta_1)u_-^2}{\Delta_1^2\left(\Delta_1^2-1\right)^2}\left[u_{12}^2\left(\Delta_1^2+1\right)+2\Delta_1 u_{12,\parallel}^2\right]. \tag{4.27}$$

While the above expressions (4.26) and (4.27) for $M = 0,1$ are applicable for $u_{12} \sim u_-$, in general the expansion in Eqs. (4.24) and (4.25) is legitimate only for $u_{12} \ll u_-$ as all terms $O(u_{12}^k)$ with $k > 2$ are neglected. As we show next, higher-order corrections $O(u_{12}^k)$, $k > 2$, to Γ_n become relevant starting from transitions with $M = 2$. In particular, full expression for the contribution $\Gamma_0^{(2)}$ in Eq. (4.24) contains a correction $\propto u_{12}^6$; see Eq. (4.31) below.

D. Hybridized polaronic states and energy relaxation for $u_{12} \sim |\mathbf{u}_{11} - \mathbf{u}_{22}|$

The above results were obtained for the weak-coupling regime, $u_{12} \ll |\mathbf{u}_{11} - \mathbf{u}_{22}|$. In this limit, it is sufficient to retain the first-order terms $O(u_{12})$ in the multiphonon matrix element $\langle\Psi_{1\mu}|\mathbf{x}|\Psi_{2\nu}\rangle$. In the case $u_{12} \sim |\mathbf{u}_{11} - \mathbf{u}_{22}|$ one needs to take into account higher-order terms. The exact solution (2.9) for the polaronic states of isolated levels is not particularly useful in this case, and one needs to apply ordinary high-order perturbation theory to approximate the mixed polaronic states $\Psi_{k\mu}$. Alternatively, using numerical methods [16–18] it is not difficult to calculate the matrix element $\langle\Psi_{1\mu}|\mathbf{x}|\Psi_{2\nu}\rangle$ to any

desired order in the electron-phonon coupling, as the problem reduces to diagonalization of the system consisting of 2LS coupled to two oscillators (4.16) and (4.17).

Here we perform an analytical treatment, and therefore restrict ourselves to the simplest case of third-order corrections $O(u_{12}^3)$. To this end, we put $\mathbf{u}_{11} = \mathbf{u}_{22} = 0$, and calculate $\Psi_{k\mu}$ up to order $O(u_{12}^3)$. [Since u_{12} represents the interlevel interaction in Eq. (2.2), only odd powers of u_{12} can appear in the interlevel matrix element $\langle\Psi_{1\mu}|\mathbf{x}|\Psi_{2\nu}\rangle$. Also, as we put $\mathbf{u}_{11} = \mathbf{u}_{22} = 0$, the only relevant $\mathcal{X}$-phonon mode is that generated by $\mathbf{u}_{12}$.] The resulting matrix element (where we keep terms $\propto u_{12}^3$ only) is given by

$$\langle\Psi_{1\mu}|\mathbf{x}|\Psi_{2\nu}\rangle = \mathbf{u}_{12}u_{12}^2 X_{\mu\nu},$$

$$X_{\mu\nu} = \sum_{lmk} x_{\mu l}x_{lm}x_{mk}x_{k\nu}\left\{\frac{1}{\Delta_{\nu-k}}\left[\frac{\delta_{m\nu}}{\Delta_{\nu-l}^2} + \left(\frac{1}{\Delta_{\nu-l}} - \frac{1}{\Delta_{l-\mu}}\right)\left(\frac{1-\delta_{\nu m}}{\nu-m} - \frac{\delta_{\nu m}}{2\Delta_{\nu-k}}\right)\right] - \frac{1}{\Delta_{l-\mu}}\left[\frac{\delta_{m\mu}}{\Delta_{k-\mu}^2} + \left(\frac{1}{\Delta_{k-\mu}} - \frac{1}{\Delta_{\nu-k}}\right) \times \left(\frac{1-\delta_{m\mu}}{m-\mu} - \frac{\delta_{m\mu}}{2\Delta_{l-\mu}}\right)\right]\right\}. \quad (4.28)$$

Here $x_{\mu\nu} = \langle\mu|x|\nu\rangle = \delta_{\mu,\nu+1}\sqrt{\mu/2} + \delta_{\nu,\mu+1}\sqrt{\nu/2}$. Similar to the case considered in two preceding subsections, terms corresponding to the maximal possible change of phonon occupation number ($|\nu-\mu| = 4$ in this particular case) cancel out due to destructive interference. As a result, nonzero $\langle\Psi_{1\nu+4}|\mathbf{x}|\Psi_{2\nu}\rangle$ appears at order u_{12}^5 or $u_{12}^3u_{kk}^2$, with corresponding relaxation rate proportional to the tenth power of electron-phonon coupling. In view of $u_{kl} \ll 1$, the case $|\nu-\mu| \geqslant 4$ is barely important for applications.

Corrections of order u_{12}^3 to the terms with $M = |\nu-\mu| < 2$ in Eqs. (4.21) and (4.22) can be neglected; see Eqs. (4.26) and (4.27). Equation (4.28) with $\mu = 2$ and $\nu = 0$ provides a correction $O(u_{12}^6)$ to $\Gamma_0^{(2)}$ entering Eq. (4.24). The matrix element (4.28) is written in the single-mode basis produced by $\mathbf{u}_{12}$. In the basis (4.16)–(4.18) it generates three matrix elements,

$$\begin{aligned}\langle\Psi_{1,2,0}|\mathbf{x}|\Psi_{2,0,0}\rangle &= \mathbf{u}_{12}u_{12,\parallel}^2 X_{20},\\ \langle\Psi_{1,1,1}|\mathbf{x}|\Psi_{2,0,0}\rangle &= -\sqrt{2}\mathbf{u}_{12}u_{12,\parallel}u_{12,\perp}X_{20},\\ \langle\Psi_{1,0,2}|\mathbf{x}|\Psi_{2,0,0}\rangle &= \mathbf{u}_{12}u_{12,\perp}^2 X_{20},\end{aligned} \quad (4.29)$$

which should be added to the corresponding matrix elements in Eq. (4.24). Here X_{20} is given by Eq. (4.28),

$$X_{20} = \frac{\sqrt{2}}{\Delta_1}\left(\frac{1}{\Delta_1^2} + \frac{1}{\Delta_1^2-1} + \frac{2}{\Delta_1^2-4}\right). \quad (4.30)$$

The resulting full expression for $\Gamma_0^{(2)}$ valid for $u_{12} \sim u_- \ll 1$ reads ($\Delta_2 = E-2 = \Delta_1 - 1$)

$$\Gamma_0^{(2)} = 2w(\Delta_2)\left\{u_{12}^2u_{12,\perp}^4X_{20}^2 + 2u_{12,\parallel}^4u_{12,\perp}^2X_{20}^2 + \left[\frac{u_{12,\perp}u_-^2}{2\Delta_2(\Delta_2^2-1)} - \sqrt{2}u_{12,\parallel}u_{12,\perp}^2X_{20}\right]^2 + \left[\frac{u_{12,\parallel}u_-^2}{2^{3/2}(\Delta_2^2-1)}\left(1+\frac{2}{\Delta_2}\right) + u_{12,\parallel}^3X_{20}\right]^2 + \left[\frac{u_{12,\perp}u_-^2}{2^{3/2}(\Delta_2^2-1)} + u_{12,\parallel}^2u_{12,\perp}X_{20}\right]^2\right\}. \quad (4.31)$$

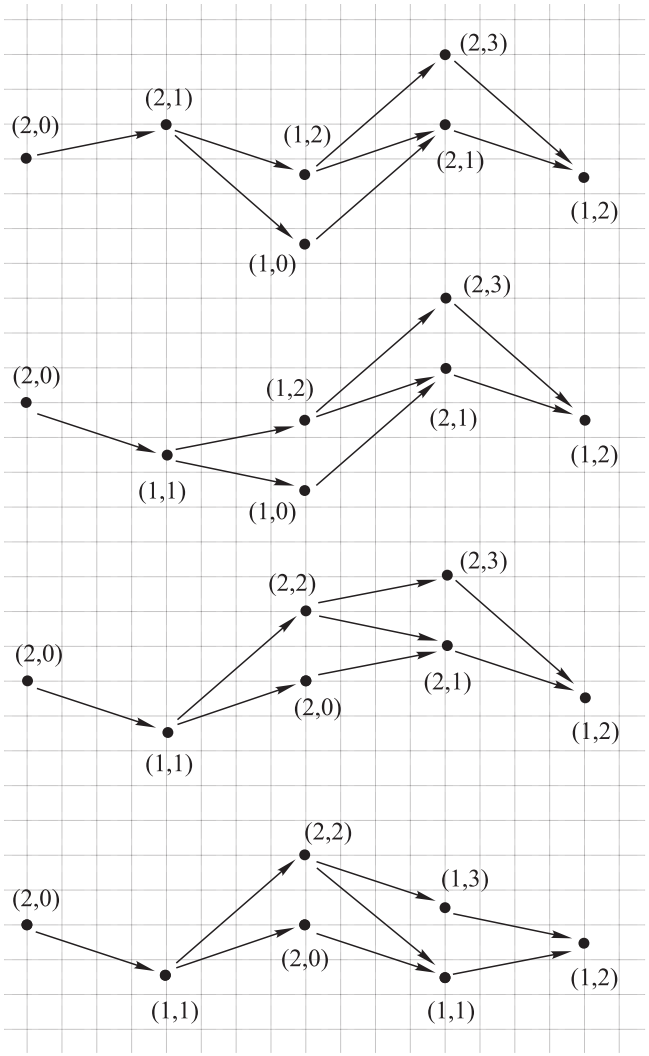

FIG. 2. Graphical representation of the matrix element $\langle\Psi_{1,2}|\mathbf{x}|\Psi_{2,0}\rangle$, Eq. (4.28), illustrating 12 quantum paths connecting states (2,0) and (1,2) via different intermediate virtual states for $E = 5/2$. The vertical distance between the states (n,k) and (m,l) represents their energy separation in units $\hbar\Omega$.

Below we discuss the part of this expression which remains in the limit $u_- \to 0$,

$$\Gamma_0^{(2)}|_{u_-=0} = 2w(\Delta_2)u_{12}^6X_{20}^2. \quad (4.32)$$

It can be easily obtained from Eq. (4.28) in the original single-mode representation generated by $\mathbf{u}_{12}$. Figure 2 illustrates interference of the amplitudes involving different intermediate phonon states which enter the corresponding matrix element $\langle\Psi_{1\nu+2}|\mathbf{x}|\Psi_{2\nu}\rangle$. Three out of four matrix elements $x_{\mu\nu}$ entering Eq. (4.28) arise from the interlevel interaction $\mathbf{u}_{12}\cdot\mathbf{x}$ which leads both to a change of the electronic index and the phonon occupation number. The remaining $x_{\mu\nu}$ originates from the

anharmonic interaction which changes the phonon occupation number but not the electronic index. Depending on the order of these operators, 4 groups of quantum paths appear in Fig. 2. Each group consists of 3 paths connecting different intermediate phonon states.

V. ENERGY RELAXATION IN VICINITY OF RESONANCES

In the previous section we developed a systematic approach to multiphonon transitions using perturbation theory, which relies on smallness of both the couplings between levels of two polaronic ladders and the anharmonic interaction with respect to separation between the levels. This approach should be modified in vicinity of resonances, where certain energy denominators entering Eqs. (4.24)–(4.26) become close to zero. What kind of modification is required depends on the relation between the tunnel couplings of resonant levels $t\Omega$ and the anharmonic decay rate w. In the limiting case $t\Omega \gg w$, Sec. V A, one should take into account the avoided crossing of resonant levels while the anharmonic interaction can still be treated perturbatively using the golden-rule approximation (3.3). Due to the avoided crossing, the separation of levels entering Eqs. (4.24)–(4.26) near the resonance is of order $t\Omega$. Accordingly, the relaxation rate is roughly w since it is determined by the weak anharmonic decay of strongly coupled states. In the opposite limit $t\Omega \gg w$, Sec. V B, fast intraladder transitions suppress the coherent interladder dynamics, and the relaxation rate at the resonance becomes of the order of $t^2\Omega^2/w$.

A. Strong-coupling regime, $t\Omega \gg w$

We consider the vicinity of the resonance $E = K$ with integer $K \geqslant 1$ at low temperature, $T \ll \hbar\Omega$. Near the resonance the energy relaxation is dominated by the term $M = K - 1$ in Eq. (4.24), corresponding to $\Delta_M \simeq 1$. Indeed, the terms $M = K \pm 2$ ($\Delta_M \simeq \mp 2$) are irrelevant as the corresponding energy denominators do not vanish at the resonance. The term $M = K$ does not lead to energy relaxation. Finally, the processes $M = K + 1$ are exponentially suppressed since for $\Delta_{K+1} \simeq -1$ they require absorption of large energy from the bath, $w(-1) = \exp(-\hbar\Omega/T)w(1)$.

The main term $M = K - 1$ is dominated by processes involving coupling of the level $|l\rangle = |\phi_{2,0,0}\rangle$ to degenerate levels $|r_\parallel\rangle = |\phi_{1,K,0}\rangle$ and $|r_\perp\rangle = |\phi_{1,K-1,1}\rangle$, as illustrated in Fig. 3(a). Neglecting the irrelevant off-resonant processes [shown in Figs. 3(c) and 3(d)], we rewrite Eq. (4.24) in the vicinity of $E = K$ as

$$\Gamma_0|_{w(1),\,t_\parallel,\,t_\perp \ll |\Delta_K| \ll 1} = Kw(1+\Delta_K)\frac{t^2}{\Delta_K^2}, \tag{5.1}$$

where

$$t^2 = |t_\parallel|^2 + |t_\perp|^2 \tag{5.2}$$

represents the tunnel couplings between the resonant states,

$$t_\parallel = \langle l|\mathbf{u}_{12}\cdot\mathbf{x}|r_\parallel\rangle = \frac{u_-^{K-1}u_{12,\parallel}\sqrt{K!}}{2^{K/2}(K-1)!},$$
$$t_\perp = \langle l|\mathbf{u}_{12}\cdot\mathbf{x}|r_\perp\rangle = \frac{u_-^{K-1}u_{12,\perp}\sqrt{(K-1)!}}{2^{K/2}(K-1)!}. \tag{5.3}$$

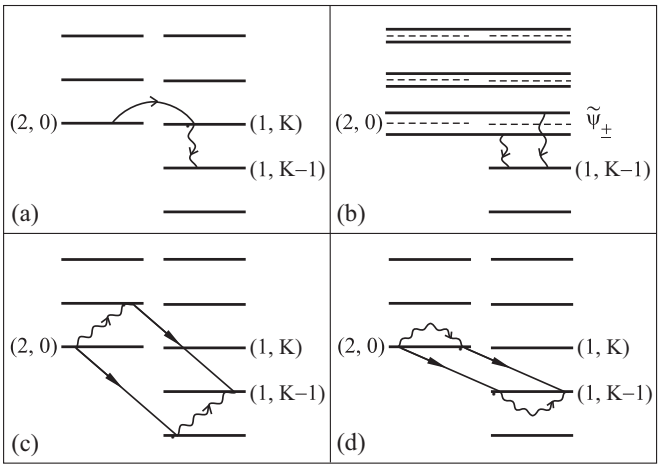

FIG. 3. Resonant coupling of the polaron states (2,0) and (1,K) [panel (a)] leads to their mixing and splitting [panel (b)]. Note that (1,K) includes several degenerate states, in particular, $|r_\parallel\rangle = |\phi_{1,K,0}\rangle$ and $|r_\perp\rangle = |\phi_{1,K-1,1}\rangle$. Panels (c) and (d) illustrate two off-resonant terms in Eq. (4.24) for $M = K - 1$ which can be ignored in the vicinity of the resonance.

Provided $w(1) \ll t\Omega$ (the opposite limit is considered in Sec. V B), at $|\Delta_K| \lesssim t$ one should take into account strong mixing and splitting of the resonant states. Let ε_s and $\widetilde{\Psi}_s = C_{sl}|l\rangle + C_{s\parallel}|r_\parallel\rangle + C_{s\perp}|r_\perp\rangle$ be eigenvalues and normalized eigenvectors of the corresponding tunneling Hamiltonian,

$$\begin{pmatrix} \Delta_K - \varepsilon_s & t_\parallel & t_\perp \\ t_\parallel^* & -\varepsilon_s & 0 \\ t_\perp^* & 0 & -\varepsilon_s \end{pmatrix}\begin{pmatrix} C_{sl} \\ C_{s\parallel} \\ C_{s\perp} \end{pmatrix} = 0. \tag{5.4}$$

The rate of anharmonicity-induced transitions from $\widetilde{\Psi}_s$ to the low-lying states $|\phi_{1,K-1,0}\rangle$ and $|\phi_{1,K-2,1}\rangle$ (not modified near the resonance) is given by Eq. (3.3),

$$\begin{aligned}\widetilde{\Gamma}_s &= 2w(1+\varepsilon_s)\big[C_{s\parallel}^2\,\langle\phi_{1,K-1,0}|\mathbf{x}|r_\parallel\rangle^2 \\ &\quad + C_{s\perp}^2\,\langle\phi_{1,K-1,0}|\mathbf{x}|r_\perp\rangle^2 + C_{s\perp}^2\,\langle\phi_{1,K-2,1}|\mathbf{x}|r_\perp\rangle^2\big] \\ &= Kw(1+\varepsilon_s)\big[C_{s\parallel}^2 + C_{s\perp}^2\big].\end{aligned} \tag{5.5}$$

Among the eigenstates $\widetilde{\Psi}_s$, the one with zero eigenvalue $\varepsilon_0 = 0$ is decoupled from the left ladder state $|l\rangle$. The decay of the corresponding eigenstate,

$$\widetilde{\Psi}_0 = t^{-1}(t_\perp|r_\parallel\rangle - t_\parallel|r_\perp\rangle), \tag{5.6}$$

represents the rate of intraladder relaxation,

$$\widetilde{\Gamma}_0 = Kw(1), \tag{5.7}$$

and does not change across the resonance.

The left ladder state $|l\rangle$ couples to the combination $|r\rangle = t^{-1}(t_\parallel^*|r_\parallel\rangle + t_\perp^*|r_\perp\rangle)$ of the right ladder states yielding two remaining eigenstates of Eq. (5.4),

$$\widetilde{\Psi}_\pm = \frac{\varepsilon_\pm|l\rangle + t|r\rangle}{(\varepsilon_\pm^2 + t^2)^{1/2}}, \tag{5.8}$$

with eigenenergies

$$\varepsilon_\pm = \Delta_K/2 \pm \sqrt{\Delta_K^2/4 + t^2}; \tag{5.9}$$

see Figs. 3(a) and 3(b). It is worth recalling here that the polaron shifts $u_{kk}^2/2$ are already included in the definition of Δ_K; see Eq. (4.2).

According to Eq. (5.5), the energy relaxation rate from the states $\widetilde{\Psi}_\pm$ reads

$$\widetilde{\Gamma}_\pm = Kw(1+\varepsilon_\pm)\frac{t^2}{\varepsilon_\pm^2+t^2}. \tag{5.10}$$

Similar results for the lowest-order resonance $K=1$ were obtained in Refs. [26,27].

Exactly at the resonance $\Delta_K=0$, Eq. (5.9) yields $\varepsilon_\pm=\pm t$; relaxation rates (5.10) reach the maximal value

$$\widetilde{\Gamma}_\pm = Kw(1\pm t)/2. \tag{5.11}$$

This result has a simple physical interpretation: Exactly at the resonance, the electron spends on average half of its time in the right-ladder states, where it can decay to the lower states with the rate $Kw(1\pm t)$; see also Refs. [25,27].

At large positive detuning from the resonance, $t \ll \Delta_K \ll 1$, the states $\widetilde{\Psi}_+$ and $\widetilde{\Psi}_-$ evolve correspondingly into $|l\rangle$ and $|r\rangle$. Accordingly, the rate $\widetilde{\Gamma}_+$ transforms into its asymptotic form (5.1), while $\widetilde{\Gamma}_-$ transforms into the rate of intraladder transitions (5.7). At large negative detuning the behavior is the same up to interchange of indices $+$ and $-$.

B. Incoherent resonant tunneling, $t\Omega \ll w$

The theory presented above is valid for $t\Omega \gg w(1)$. In typical self-organized QDs this condition is usually met for $K=1$ [26,27]. In the vicinity of higher-order resonances, the opposite condition $t\Omega \ll w(1)$ is satisfied starting from some K since $t \propto u_-^{2(K-1)}$ with $u_- \ll 1$. When $t\Omega \ll w(1)$, Eq. (5.1) correctly describes the energy relaxation for Δ_K in the region $w(1)/\Omega \ll \Delta_K \ll 1$. At smaller detuning the golden-rule approximation (3.3) fails, and Eq. (5.1) should be modified in the following way:

$$\Gamma_0 = Kw(1+\Delta_K)\frac{t^2}{\Delta_K^2+[\,Kw(1)/2\Omega\,]^2}. \tag{5.12}$$

Below we obtain this result by solving the equation

$$i(\partial_\tau + G)\rho = [H,\rho] \tag{5.13}$$

for the density matrix ρ reduced to two resonant states $|1\rangle = |l\rangle$ and $|2\rangle = |r\rangle$, specified in the previous subsection.

Here H is the reduced form of the tunneling Hamiltonian (5.4),

$$H = \begin{pmatrix} \Delta_K & t \\ t & 0 \end{pmatrix}, \tag{5.14}$$

and τ is the dimensionless time (in units of Ω^{-1}). The relaxation matrix

$$G = \begin{pmatrix} 0 & \gamma_{nd} \\ \gamma_{nd} & \gamma \end{pmatrix} \tag{5.15}$$

accounts for the anharmonic decay of optical phonons in the state $|r\rangle$, given by $\gamma = Kw(1)/\Omega$, and for the decoherence associated with this anharmonic decay, $\gamma_{nd} = \gamma/2$. The physical reason for γ_{nd} being twice smaller than γ_d is the same as in Eq. (5.11) above. The quantity γ_{nd} describes the rate of decay of the Rabi oscillations between two resonant states. The polaron can escape from one of these states with probability γ while the other state in the absence of tunneling is everlasting. Diagrams for ρ_{12} and ρ_{22}, illustrating the relation $\gamma_{nd} = \gamma/2$, are sketched in Figs. 4(a) and 4(b).

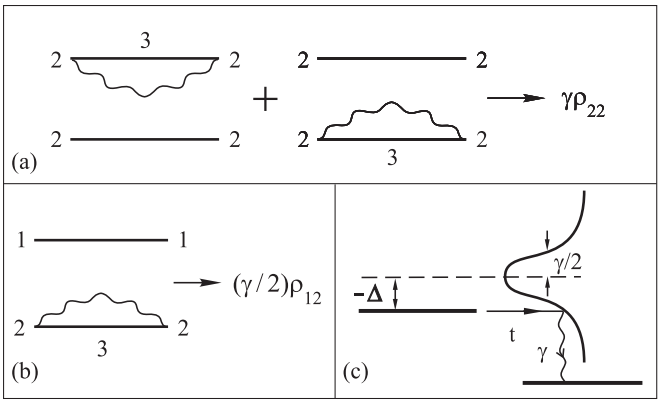

FIG. 4. Diagrammatic illustration of the relation $\gamma = 2\gamma_{nd}$ between the longitudinal [γ, panel (a)] and the transverse [γ_{nd}, panel (b)] relaxation rate in the situation when the state 1 is everlasting, while the state 2 decays with probability γ to the third state 3. Panel (c): An equivalent description in terms of incoherent tunneling is applicable when the level width γ exceeds the Rabi frequency t.

Imposing the initial condition $\rho_{11}(\tau=0)=1$ and using the Laplace transform of the density matrix equation (5.13),

$$i(s+G)\rho(s) = [H,\rho(s)] + |1\rangle\langle 1|, \tag{5.16}$$

one obtains a general solution in the form

$$\begin{aligned} \rho_{11} &= [\,s+\gamma+\tilde{t}^2(s)\,]D^{-1}(s), \\ \rho_{22} &= \tilde{t}^2(s)\,D^{-1}(s), \\ \tilde{t}^2(s) &= \frac{2t^2(s+\gamma_{nd})}{(s+\gamma_{nd})^2+\Delta_K^2}, \\ D(s) &= s[\,s+\gamma\,]+\tilde{t}^2(s)[\,2s+\gamma\,]. \end{aligned} \tag{5.17}$$

Equation (5.17) is valid for arbitrary relation between Δ_K, t, and γ. It describes incoherent dynamics of a system driven by the interplay of Rabi oscillations and anharmonic decay. The notion of the energy relaxation rate is not well defined at $t \sim \gamma$ as the decay is not exponential. The exponential law is restored at $\gamma \gg t$. In this case, $\rho_{22} \ll \rho_{11}$ at all times due to the rapid decay of the state $|r\rangle$; the solution (5.17) can be approximated as

$$\rho_{11}(s) = (s+\alpha)^{-1}, \quad \alpha = \frac{2t^2\gamma_{nd}}{\gamma_{nd}^2+\Delta_K^2}. \tag{5.18}$$

Equation (5.18) yields $\rho_{11}(\tau) = \exp(-\alpha\tau)$. Using $\gamma_{nd} = \gamma/2 = Kw(1)/2\Omega$ we see that the decay rate $\alpha\Omega = Kw(1)t^2/(\gamma_{nd}^2+\Delta_K^2)$ coincides with the expression (5.12) [Δ_K in the argument of w in Eq. (5.12) is important only away from the resonance, for $|\Delta_K| \gg \gamma$].

The same result can be obtained by considering the tunneling from a discrete level $|l\rangle$ to a strongly broadened level $|r\rangle$ with the density of states $\nu(\varepsilon) = -\pi^{-1}\mathrm{Im}(\varepsilon + i\gamma/2)^{-1}$; see Fig. 4(c). In the state $|r\rangle$ the polaron immediately relaxes to the

lower energy states. The tunneling rate $W = 2\pi\Omega|t|^2\nu(\Delta_K)$ obtained in this way coincides with the inelastic scattering rate (5.12).

Using the above approach, we now estimate the high-T incoherent tunneling rate. At $T \neq 0$, the n-phonon state $|i,n\rangle$ of the ladder i can decay into either of the neighboring states $|i,n \pm 1\rangle$ by emitting $(-)$ or absorbing $(+)$ the bath phonons; the probability of the escape is $\gamma_n = nw(1) + (n+1)w(-1)$. At $T = 0$ the rate $w(-1) = 0$ and we return to the result above. Considering now two resonant levels $|i,n\rangle$ and $|f,m\rangle$ of different ladders whose mutual coupling $|t| \ll \gamma_{n,m}$ is small compared to their width, we obtain for the tunneling rate $W(\Delta) = 2\pi\Omega|t|^2 \int d\varepsilon \nu_n(\varepsilon)\nu_m(\varepsilon+\Delta)$, where $\nu_k(\varepsilon) = -\pi^{-1}\mathrm{Im}(\varepsilon + i\gamma_k/2)^{-1}$. The result can be expressed as $W = 2\pi\Omega|t|^2\tilde{\nu}(\Delta)$ with $\tilde{\nu}(\Delta) = \bar{\gamma}/\pi(\Delta^2 + \bar{\gamma}^2)$. The effective transverse relaxation rate, $\bar{\gamma} = (\gamma_n + \gamma_m)/2$, determines the width of resonances in Eq. (4.25) in the incoherent tunneling regime; see Sec. VI.

VI. ILLUSTRATION AND DISCUSSION OF RESULTS

Here we first illustrate our results for a specific channel of anharmonic interaction and then discuss their qualitative features and possible generalizations. For illustration we use a phenomenological description of the anharmonic channel where the $\mathcal{X}$ phonon decays into two longitudinal acoustic (LA) phonons. Namely, we introduce the function $w(\Delta)$, defined in Eq. (3.4), in the form

$$w(\Delta) = w_0(1)\tilde{F}(\Delta)[1 - \exp(\Delta/2T)]^{-2}. \tag{6.1}$$

Here $\tilde{F}(\Delta) = F(\Delta)/F(1)$, while the function F is

$$F(\Delta) = \frac{\Delta^4(|\Delta| - \Delta_{\max})^2}{10^{-2}\Delta_{\max}^2 + (|\Delta| - \Delta_{\max})^2} \tag{6.2}$$

for $|\Delta| < \Delta_{\max}$ and zero otherwise. In Eq. (6.1), $w_0(1) = w(1)|_{T=0}$ is the value of anharmonic decay of the LO phonon in the bulk material at zero temperature (as before, we measure all energies in units of LO phonon energy). The dimensionless function $\tilde{F}(\Delta)$ describes the $T = 0$ dependence of anharmonic matrix elements and of the available phase space on the energy $\Delta/2$ of emitted LA phonons, and the last factor in Eq. (6.1) originates from the thermal factors $\mathcal{N}_k$ in Eq. (3.4). The T-dependence takes into account that in the chosen channel two LA phonons with equal energy $|\Delta|/2$ and opposite momenta are either emitted ($\Delta > 0$) or absorbed ($\Delta < 0$); see Fig. 5. The dependence (6.2) is chosen on phenomenological grounds. It assumes that $w(\Delta) \propto \Delta^4$ at $\Delta \ll 1$, [27] and that the maximal value of the transferred energy $\Delta_{\max}$ is twice the maximal energy of the LA phonon. The angular dispersion of the spectrum of acoustic modes near the boundary of the Brillouin zone is modeled via the 10% dispersion of $\Delta_{\max}$.

For numerical estimates we take the parameters typical for self-organized QDs in a GaAs matrix [13,14,16,19–27]. We take $u_{12,\perp}^2 = u_{12,\parallel}^2 = u_-^2 = 0.01$ for the coupling with $\mathcal{X}$-phonon modes, $w_0(1) = 0.002\,\Omega = (9\ \mathrm{ps})^{-1}$ for the $T = 0$ anharmonic decay rate of the LO phonon in bulk GaAs [30], $\hbar\Omega = 36$ meV for the LO phonon energy, and $\hbar\omega_{\max} = 27$ meV for the maximal energy of LA phonon, which gives $\Delta_{\max} = 54/36$ in Eq. (6.2).

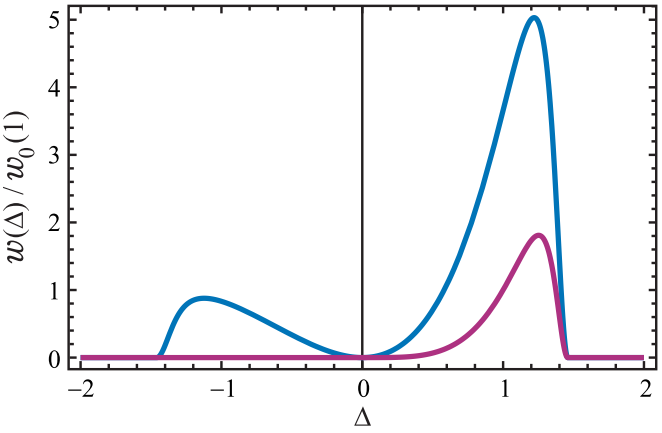

FIG. 5. (Color online) The anharmonic decay rate $w(\Delta)$, Eq. (6.1) [in units of $w_0(1)$], vs the energy Δ transferred to the bath (in units of the LO phonon energy $\hbar\Omega$) for $T = 0$ (lower line) and $T = 300$ K (upper line).

The inelastic relaxation rate at $T = 0$ is illustrated in Fig. 6 where we interpolate the results obtained using different methods away and close to the resonances $E \simeq 1,2,3,\ldots$. The dashed lines represent the off-resonant results (4.26), (4.27), and (4.31), where E is given by Eq. (4.2). As expected from Eq. (4.24), outside the resonances the rate falls approximately as $\Gamma(E+1)/\Gamma(E) \sim u^2 = 10^{-2}$ with the increase of the transition energy by the LO phonon energy. This behavior is the result of quantum interference between processes involving different virtual polaron states, as detailed in Sec. IV. The situation near the maxima $E \simeq 1,2,3,\ldots$ is quite different. For our choice of parameters, the anticrossing $2t_1 = \sqrt{2}|u_{12}| = 0.2$ of levels at $E \simeq 1$ is two orders of magnitude larger than their width $\gamma_{\mathrm{nd}} = w_0(1)/2\Omega = 0.001$. Accordingly, the energy relaxation rate (4.26) is modified as described in Sec. V A. In particular, it takes the maximal value $\tilde{\Gamma}_\pm \simeq w_0(1 \pm t_1)/2$ at $E = 1 \pm t$; see Eq. (5.11). Note that the values $w(1+t)$ and $w(1-t)$ for such a large $t \sim 0.1$ can be appreciably different [27]. Near $E \simeq 2$ the splitting

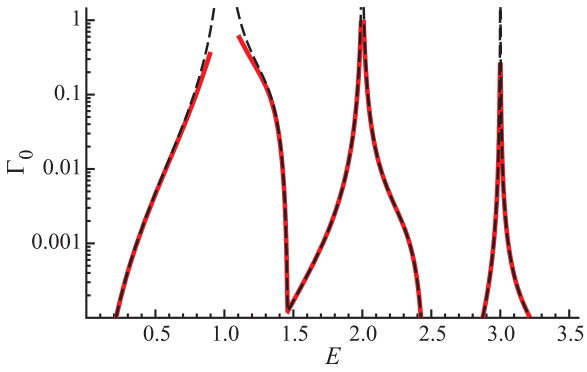

FIG. 6. (Color online) The inelastic relaxation rate [in units of $w_0(1)$] vs the separation E of the lowest polaron levels in two ladders (in units of LO phonon energy) for $T = 0$. The dashed lines illustrate the off-resonant results (4.26), (4.27), and (4.31) where E is given by Eq. (4.2). Solid line: the anticrossing of the resonant levels near $E = 1$ and $E = 2$, Sec. V A, and the anharmonicity-induced broadening of levels near $E = 3$, Sec. V B, are taken into account.

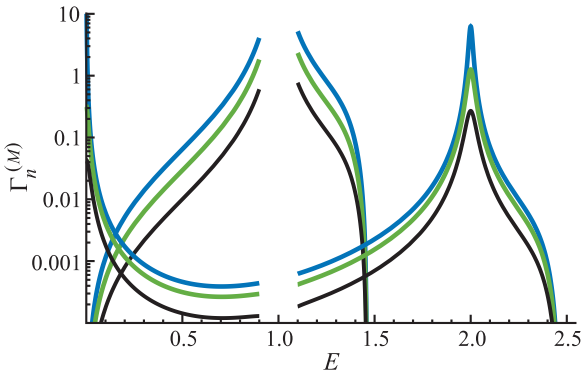

FIG. 7. (Color online) Contributions $\Gamma_n^{(M)}$ of different channels to the inelastic relaxation rate Γ_T, Eq. (4.25), at $T = 300$ K as a function of the level separation E. Different curves correspond to $n = 0,1,2$ (from top to bottom) and to $M = 0$ (curves peaked at $E \sim 1$) and $M = 1$ (peaked at $E \sim 2$ and $E \sim 0$). The corrections to Eq. (4.25) near $E = 2$ due to anharmonicity-induced broadening of levels, Sec. V B, are taken into account.

of resonant levels $2t_2 = \sqrt{(u_{12,\perp}^2 + 2u_{12,\parallel}^2)u_-^2} \simeq 0.016$ is still larger than $\gamma_{\rm nd} = 2w_0(1)/2\Omega = 0.002$. The gap $2t_2$ in the spectrum is quite small compared to $2t_1$, and the maximal values of the inelastic rate in two branches are practically the same, $\tilde{\Gamma}_+ \simeq \tilde{\Gamma}_- \simeq w_0(1)$. Finally, at $E \simeq 3$ the anticrossing becomes smaller than $\gamma_{\rm nd} = 3w_0(1)/2\Omega$, and the results of Sec. V B for the incoherent tunneling regime apply.

The temperature evolution of the relaxation rate is illustrated in Figs. 7 and 8. As discussed in Sec. IV C, at finite temperature one should take into account the nonzero thermal occupation of excited states in the upper polaron ladder since the intraladder thermalization is generally much faster than the multiphonon interladder transitions. The contribution Γ_n of these excited states to the inelastic relaxation (4.25) is shown in Fig. 7 for zero-, one-, and two-phonon occupation of the initial polaron state ($n = 0,1,2$). For each channel n, the contributions of $M = 0$ (peaked near $E = 1$) and of $M = 1$ (peaked near $E = 2$ and $E = 0$) in Eq. (4.25) are shown separately. Note that the nonzero contribution of the $M = 1$ term at $E < 1$ appears at $T \neq 0$ only. It is associated with the possibility to take energy from the phonon bath at $T > 0$ which leads to a finite $w(\Delta)$ for $\Delta < 0$; see Fig. 5. Apart from

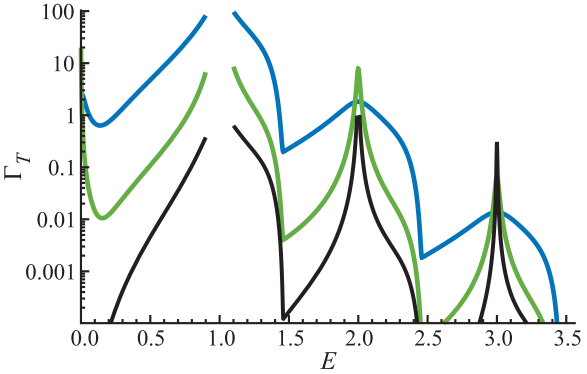

FIG. 8. (Color online) The inelastic relaxation rate Γ_T [in units of $w_0(1)$] vs the level separation E for $T = 0$ K, 300 K, and 1000 K (from bottom to top).

that, at elevated temperature the rate of anharmonicity-induced intraladder transitions also increases, so that at $T = 300$ K the anticrossing of levels near the resonance $E = 2$ becomes smaller than the broadening of the polaron levels; see Sec. V B. As a result, with increasing T the relaxation rate Γ_T at $E \sim 2$ first grows, since in the strong-coupling regime $\Gamma_n^{(M)} \propto w(\Delta_M)$, see Sec. V B, and then diminishes, since in the incoherent tunneling regime $\Gamma_n^{(M)} \propto w^{-1}$ in the vicinity of resonances. This behavior is clearly seen in Fig. 8. Similarly, near $E = 1$ the rate grows with T since the system remains in the strong-coupling regime, while near $E = 3$ the rate grows outside the peak and decreases at the peak position since here the system remains in the incoherent tunneling regime at all T.

On a more general level, it is seen that the perturbative approach of Sec. IV (represented by dashed lines in Fig. 6) is applicable almost everywhere away from the resonance $E \sim 1$, addressed in earlier studies of anharmonic relaxation [25–27]. As detailed above, the most interesting feature of higher resonances $E \sim K$ for $K > 1$ is the crossover from the strong-coupling regime of $E \sim 1$ to the incoherent tunneling regime with increasing K or temperature which leads, in particular, to a nonmonotonic T dependence of the $E \sim 2$ peak in Fig. 8.

The theory presented in this work assumes two nondegenerate levels while most existing theoretical works (aimed on explanation of experimental data for a particular system of self-organized QDs [14,15,19–22]) consider a 3-level model of QD involving two nearly degenerate excited p-type states on top of single s-type ground state [25–27]. For the 2-level system, we find relatively compact expressions which enable a qualitative analysis of the relevance of particular channels of relaxation in various regimes for more complex systems. Apart from that, the perturbative approach of Sec. IV demonstrates explicitly the significance of destructive interference between multiphonon processes involving different intermediate virtual states which was not properly discussed in this context before. We also mention that our 2-level model is directly applicable to transitions between states of coupled quantum dots in QCL [5] or to quantum dashes [6]. For 3 or more levels a complete analytic study similar to that in Sec. IV does not appear reasonable. At the same time, calculation of the multiphonon matrix elements entering Eq. (3.3) using numerical methods developed previously in the studies of polaron spectrum (see Refs. [16–18] and references therein) appears feasible and desirable.

It would be interesting to systematically study $w(\Delta)$ in a broad interval of Δ and T both for 3-phonon and 4-phonon anharmonic interactions which would require generalization of numerical techniques developed in Refs. [29,30]. The first steps in this direction were performed in Refs. [21,22,26,27] which proved the importance of various channels of LO 3-phonon anharmonic relaxation including LA-TA, LA-TO, and TA-LO channels [27] in addition to the LA-LA channel illustrated above. More detailed study may discover additional sharp features in $w(\Delta)$ detectable in experiment. Such features may originate from unusual channels of anharmonic interactions such as coupling of three Γ-point optical phonons which never play a role in the decay of bulk phonons studied before. In this respect, 2-level QD systems with level separation adjustable, for instance, by external voltage [5] or magnetic

field [28] may serve as a sensitive detector for a rich variety of anharmonic interactions.

VII. CONCLUSION

We calculated the multiphonon energy relaxation in a single-occupied two-level quantum dot, where the electron interacts with certain optical phonon modes which decay and transfer the transition energy to the lattice. Our theory includes the previously unexplored range of transition energies several times larger than the optical phonon energy and systematically studies the role of quantum interference of the processes involving different virtual polaron states. Analytic results are obtained both for the perturbative off-resonant regime and for the resonant regime, which can be coherent or incoherent depending on the electron-phonon and anharmonic coupling strengths, the order of the resonance, and temperature.

ACKNOWLEDGMENTS

This work was supported by the Deutsche Forschungsgemeinschaft, by the Russian Foundation for Basic Research, and by the Program on Fundamental Research in Nanotechnology and Nanomaterials of the Presidium of the Russian Academy of Sciences.

[1] Y. Arakawa and H. Sakaki, Appl. Phys. Lett. **40**, 939 (1982).
[2] R. A. Suris, in *Future Trends in Microelectronics*, NATO ASI Series E, Vol. 323, edited by S. Luryi, J. Xu, and A. Zaslavsky (Kluwer, Dordrect, 1996), p. 197.
[3] N. S. Wingreen and C. A. Stafford, IEEE J. Quantum Electron. **33**, 1170 (1997).
[4] Chia-Fu Hsu, Jeong-Seok O, P. Zory, and D. Botez, IEEE J. Sel. Top. Quantum Electron. **6**, 491 (2000).
[5] I. A. Dmitriev and R. A. Suris, Phys. Status Solidi (a) **202**, 987 (2005); Physica E **40**, 2007 (2008).
[6] V. Liverini, L. Nevou, F. Castellano, A. Bismuto, M. Beck, F. Gramm, and J. Faist, Appl. Phys. Lett. **101**, 261113 (2012).
[7] Jerome Faist, F. Capasso, D. L. Sivco, C. Sirtori, A. L. Hutchinson, and A. Y. Cho, Science **264**, 553 (1994).
[8] R. F. Kazarinov and R. A. Suris, Sov. Phys. Semicond. **5**, 707 (1971).
[9] R. Köhler, A. Tredicucci, F. Beltram, H. E. Beere, E. H. Linfield, A. G. Davies, D. A. Ritchie, R. C. Iotti, and F. Rossi, Nature (London) **417**, 156 (2002).
[10] B. S. Williams, Nat. Photonics **1**, 517 (2007).
[11] U. Bockelmann and G. Bastard, Phys. Rev. B **42**, 8947 (1990).
[12] H. Benisty, C. M. Sotomayor-Torres, and C. Weisbuch, Phys. Rev. B **44**, 10945(R) (1991).
[13] T. Inoshita and H. Sakaki, Phys. Rev. B **56**, R4355 (1997).
[14] S. Hameau, Y. Guldner, O. Verzelen, R. Ferreira, G. Bastard, J. Zeman, A. Lemaitre, and J. M. Gerard, Phys. Rev. Lett. **83**, 4152 (1999).
[15] S. Hameau, J. N. Isaia, Y. Guldner, E. Deleporte, O. Verzelen, R. Ferreira, G. Bastard, J. Zeman, and J. M. Gérard, Phys. Rev. B **65**, 085316 (2002).
[16] T. Stauber, R. Zimmermann, and H. Castella, Phys. Rev. B **62**, 7336 (2000).
[17] D. Obreschkow, F. Michelini, S. Dalessi, E. Kapon, and M.-A. Dupertuis, Phys. Rev. B **76**, 035329 (2007).
[18] P. Kaczmarkiewicz and P. Machnikowski, Phys. Rev. B **81**, 115317 (2010).
[19] J. Urayama, T. B. Norris, J. Singh, and P. Bhattacharya, Phys. Rev. Lett. **86**, 4930 (2001).
[20] S. Sauvage, P. Boucaud, R. P. S. M. Lobo, F. Bras, G. Fishman, R. Prazeres, F. Glotin, J. M. Ortega, and J. M. Gerard, Phys. Rev. Lett. **88**, 177402 (2002).
[21] E. A. Zibik, L. R. Wilson, R. P. Green, G. Bastard, R. Ferreira, P. J. Phillips, D. A. Carder, J-P. R. Wells, J. W. Cockburn, M. S. Skolnick, M. J. Steer, and M. Hopkinson, Phys. Rev. B **70**, 161305(R) (2004).
[22] E. A. Zibik, T. Grange, B. A. Carpenter, N. E. Porter, R. Ferreira, G. Bastard, D. Stehr, S. Winnerl, M. Helm, H. Y. Liu, M. S. Skolnick, and L. R. Wilson, Nat. Mater. **8**, 803 (2009).
[23] X.-Q. Li and Y. Arakawa, Phys. Rev. B **57**, 12285 (1998).
[24] X.-Q. Li, H. Nakayama, and Y. Arakawa, Phys. Rev. B **59**, 5069 (1999).
[25] O. Verzelen, R. Ferreira, and G. Bastard, Phys. Rev. B **62**, R4809 (2000).
[26] L. Jacak, J. Krasnyj, D. Jacak, and P. Machnikowski, Phys. Rev. B **65**, 113305 (2002).
[27] T. Grange, R. Ferreira, and G. Bastard, Phys. Rev. B **76**, 241304(R) (2007).
[28] A. Wade, G. Fedorov, D. Smirnov, S. Kumar, B. S. Williams, Q. Hu, and J. L. Reno, Nat. Photonics **3**, 41 (2009).
[29] A. Debernardi, Phys. Rev. B **57**, 12847 (1998).
[30] H. Hamzeh and F. Aniel, J. Appl. Phys **109**, 063511 (2011).
[31] Yu. E. Perlin, Sov. Phys. Usp. **6**, 542 (1964) [Usp. Phys. Nauk **80**, 553 (1963)].
[32] V. N. Abakumov, V. I. Perel, and I. N. Yassievich, *Nonradiative Recombination in Semiconductors* (North-Holland, Amsterdam, 1991).
[33] A. S. Ioselevich and E. I. Rashba, in *Quantum Tunneling in Condensed Media*, edited by Yu. Kagan and A. J. Legett (North-Holland, Amsterdam, 1992).
[34] S. V. Goupalov, R. A. Suris, P. Lavallard, and D. S. Citrin, IEEE J. Sel. Top. Quantum Electron. **8**, 1009 (2002).
[35] E. A. Muljarov and R. Zimmermann, Phys. Rev. Lett. **93**, 237401 (2004).